Advanced Mechanical Design, University of Rochester
Final Design Report
Spring 2024

LIGHT RELAY APPARATUS FOR THE LABORATORY FOR LASER ENERGETICS

Adam Cummings **Julie Hernandez** **Alex Kulvivat** **Mokin Lee** **Edban Watt**

ABSTRACT

High-energy-density phenomena are not fully understood yet by the scientific community. The Laboratory of Laser Energetics at the University of Rochester seeks to amend this gap by conducting experiments regarding the optical reflectivity of such substances. A light relay apparatus was designed and manufactured to assist with these experiments, such that light could be relayed from a backlighter sample to an experimental sample from which the reflectivity would be measured. This apparatus performed successfully in the experiment, prompting usage in future experiments, albeit with the potential for revisions to simplify the manufacturing process.

PROBLEM DEFINITION

The Laboratory of Laser Energetics (LLE) at the University of Rochester conducts research in high-energy-density (HED) phenomena. HED refers to high pressure and temperatures, achieved at the LLE by hitting a substance with lasers to shock the material into a state of HED. The LLE intends to conduct experiments on HED materials, in particular hydrogen, to measure their optical reflectivity spectrum. Previous experiments have been undertaken to measure the optical properties of solid samples. However, hydrogen, being a gas, cannot be studied in the same way. It must first be pre-compressed in a device such as a diamond anvil cell (DAC). Therefore, changes to existing platforms must be made to make them compatible with hydrogen and other gases.

The experiment connected with this project will utilize the Omega-EP laser system (fig. 1) to shoot both a sample of hydrogen compressed in a diamond anvil cell (DAC) and a backlight material to generate a broadband light source. The team is tasked with developing a mechanical apparatus to relay the light from the backlight to the HED sample so that the reflected light can be measured to understand the reflectivity of the sample. The system, dubbed the reflectivity box, will fundamentally consist of a mirror and a beam splitter (fig. 2). The reflectivity box will be mounted onto the front plate of a PXRDIP box (fig. 3), whereas the front plate and rear plate can be modified. The reflected light exiting from the rear plate will be relayed to a spectrometer to gauge the reflectivity of the HED hydrogen sample.

REQUIREMENTS, SPECIFICATIONS, DELIVERABLES

This project's completion will be defined in terms of several major deliverables, which are different tangible and intangible outputs of the project produced to be delivered to the sponsor and the course instructor. The major deliverables in completing the project are listed in Table 1.

The design requirements outline the functionality, design constraints at component interfaces, and provide the basis for choosing the manufacturing method and material involved in creating the final functioning prototype. The requirements for the final working prototype are as follows:

- The device must be mountable on an existing PXRDIP box
- The device must be compatible with both glue-on samples and screw-on DACs
- The device must allow light a path out to the spectrometer
- The device must allow a mountable shield between the back-lighter and the hydrogen sample
- The device must be align-able within the OMEGA-EP chamber
- All materials used must be vacuum compatible
- No large air bubbles may exist within the setup
- The device must relay light from the back-lighter to the hydrogen sample
- The device must fit into the space envelope defined by CAD

The success of the design will be determined by whether the final product meets a list of pre-defined specifications agreed upon by the sponsor, the course instructor, and the design team. Each specification includes both a method of evaluation and a numerical target value that must be met. The specifications for the final product of this project are listed in Table 2.

The fact that the team is to work with resources that have well-defined limits warrants the necessity of a method of project planning that explicitly lays out not only the tasks that must be done, but also the dependencies between tasks of sequential nature and the possibility of parallelization between non-sequential tasks.

How the final goal of the design project can be broken down into smaller, more specific task items is shown with a work breakdown structure (WBS). The WBS highlights the hierarchical relationship between the final goal, the sub-goals that build it, and the individual task items that build the sub-goals that all collectively define the steps involved in the project's completion. The WBS of the overall project is shown in Figure 4.

The relationship between the different task items, the necessity of sequential execution, the possibility of parallel execution, and most importantly the identification of the critical task sequence is expressed in a flowchart-like diagram called the critical path method (CPM). The CPM provides a visual representation of the dependency relationships of the individual tasks and identifies a critical path wherein the time constraints for the start and end of each task items are much more stringent. The CPM for this design project is shown in Figure 5.

CONCEPTS

The initial concepts for the reflectivity box can be seen in table 3. Concepts one through three use a lid, which allows for ease of assembly of additional components, like adding lenses or a shield; the optics were expected to be secured with small springs in a space gate. Taking concept 1 as a baseline, concept 2 differs by changing the angle of reflection from the mirror concept 3 minimizes the distance between the light source and the mirror at the cost of risking damage to the mirror, and concept 4 differs by using a backbone to hold the mirror and beam splitter in place in lieu of a small springs and forgoing the lid.

Going forward, Concept 4 was selected as the initial design for this project. Even though Concept 4 did not have the highest calculated light efficiency, it was the easiest to manufacture and assemble due to the optic mounts being held in place by a press fit instead of micro-springs. All these concepts were designed such that they could contain a lens at the beginning of the path to collimate the light to improve the light efficiency, if deemed necessary. Additionally, a shield could be added at the front of the path to protect the inside walls of the system from debris.

However, the final design (fig. 6) deviated from Concept 4 to replace the backbone by attaching the reflectivity box directly to the front plate and using tabs to secure the beam splitter and the mirror; this decision was made to eliminate the time to manufacture the backbone as well as expediate replacing the beam splitter and mirror.

MECHANICAL ANALYSIS

A tolerance analysis was performed on the hole of the tabs that interface with the 2-56 screws which fasten the tabs onto the reflectivity box, (fig. 7). In this analysis, the tolerance grade of the hole was used to determine the proper tolerance of the hole diameter on the tab. The result of the analysis determined the hole tolerance should have a max tolerance of 0.01mm and a 0mm minimum tolerance. This analysis helped influence the design of the tabs by determining how wide the tabs could be cut and understanding how accurate the positioning of the hole could be made.

A fatigue analysis was performed on the tabs, (fig. 8). The endurance limit was calculated and plotted against the Soderberg and Modified Goodman line to predict infinite or finite life. It was found from the fatigue analysis that the endurance limit was 63.8 MPa, the necessary endurance limit for modified Goodman was 1.7 MPa, and the necessary endurance limit for Soderberg was 1.7 MPa. Both modified Goodman and Soderberg Criteria predict infinite life. These results indicate the tabs will never be close to fatigue under operating conditions. This analysis confirmed the tabs are not a critical component and it is acceptable to have high variability in manufacturing quality. The results confirm large tolerances can be allowed in the design of the tab which permit quicker and cheaper fabrication.

A structural FEA linear statics analysis on the mirror tab was conducted to investigate if the tab could support the weight of the optic (fig. 9). Maximum and minimum stresses were computed to verify the tab would not deform inelastically under the weight of the optic utilizing von-mises criterion. Displacement was also measured to ensure the optic could not slip out from underneath the tab from an applied force of 0.122 N. The convergence study resulted in a maximum stress of 3.406 MPa, minimum stress of 0.001 MPa, and displacement of 8.087*10^-4 mm. The results indicate the optic can be held in place by the tab without deforming inelastically and slipping out. This analysis played a great role in computing the stresses required to perform the fatigue analysis and confirming the selection of the material was adequate.

316 Stainless Steel shim stock was selected as the material for the tabs because it can deform elastically which allows the tabs act as a spring to secure the optics. When the user bends the tabs while positioning the optic, the tab will return to its original orientation. The material is stiff enough so that while it is easy to bend, it can still support the weight of the optic with a factor of safety greater than 3. Stainless steel shim stock is very easy to form into shape during manufacturing, thin enough to cut with a shears, and punch holes for the fasteners.

A fundamental mechanical analysis was initially performed on the tabs by modeling it as a cantilever beam (fig. 10). A cantilever beam model was chosen because the tabs were designed to be fixed at one end with a force being applied on the opposite end to simulate the weight of the optics. A factor of safety of 3 on the weight of the optic was chosen and displacement was calculated to ensure the optic would be held in place if the reflectivity box was held upside down or rotated in the laser target chamber. The displacement under the applied load was calculated to be 0.000418mm Because the displacement at the end of the tab was not greater than the thickness of the optic, it was determined the tab design could secure the optic. This analysis also confirmed a 0.005in tab thickness was sufficient and other types of shim stock material could be utilized in the design of the tabs.

MANUFACTURING

The light relay system consists of several different parts. The reflectivity box was made of Aluminum 6061 and manufactured primarily on the 4 Axis CNC. The part was removed from the machine, cut roughly to size, and then the cut surface was finished to size on the CNC machine. Aluminum 6061 was selected for this part due to the relative ease of manufacturing when compared with other materials like steel, the ready availability of the material, and because the part was shielded from the laser by the front plate and therefore did not need the same robustness as some of the other parts.

The front plate was made of stainless steel 304 and initially cut to size using waterjet cutting. The edges were finished on a deburring wheel. The holes were placed in the part using a standard 3-axis mill. Stainless steel was selected for this part to resist the shock of the laser, which hit a sample located on the front plate.

The shield was also made of stainless steel 304 and cut to shape using the water jet, then deburred. The shields were then bent into shape by placing them in a vice and hitting them with a hammer. The two holes were then cut on the mill, and an endmill was used to clear out the extra space in the cutout in order to leave adequate space for the mounting of the backlighter sample. Stainless steel was selected for this part due to the necessity of shielding x rays from reaching the sample. The atomic number tends to correlate with ability to shield x rays, and the atomic number of iron is in the range of metals that could successfully shield the rays. Aluminum has too low of an atomic number and therefore would have been inadequate for this application. Copper was considered as an alternative that would have been easier to work with, but due to concerns about the cleanliness of the metal, steel was selected as the best choice.

The spacers are made of aluminum. They are made entirely on the lathe. First, the end was finished. The hole through the center was drilled before taking material off the outside to bring it down to the proper size. The spacers were then cut to size using a part splitter. Aluminum was chosen for these parts for ease of manufacturing and because there is very little load on the parts.

The tabs were made of shim stock. They were cut to size using a shear cutter. The holes were located and marked using a center punch, then cut using a stud punch. The tabs were bent into shape using a wrench. Shim stock was selected for this part so that it would be easily bent and provide the required force as a cantilever beam.

Table 4 includes the amount of time spent by each team member for manufacturing. A total of 131 hours of manufacturing went into making 8 assemblies, which means the average time to make one assembly was 16 hours and 22 minutes. However, some of the time spent on the manufacturing of the first model went into developing manufacturing plans and figuring out the best way to produce a part, or mistakes were made and the part had to be re-manufactured. Therefore, it is expected that the first part took longer than 16 hours, and the other seven were produced in less than 16 hours. The 131 hours spent manufacturing are expected to have cost $13,100 based on a cost of $100/hour.

Some of the machinery used for manufacturing has an additional cost associated with its use. This includes the 4 axis CNC machine and the waterjet cutter, which are both estimated to cost $250/hour. The program on the 4-axis CNC machine ran for 15 minutes per part. Each front plate was cut on the waterjet cutter in 23 minutes, and each shield was cut in 16 minutes, for a total of 39 minutes on the waterjet cutter per assembly. The time spent with each of the waterjet cutter and 4-axis CNC machine is summarized in table 5. The total of 432 minutes of use for these machines cost $1800.

These manufacturing costs are included in Table 6, which summarizes all the expenses associated with manufacturing. Manufacturing time of the team members was the biggest expense, followed by the purchasing of beam splitters, then machine time. Other expenses came from purchasing metal, bolts, and other materials required for the assemblies.

Team Member	**Manufacturing Time (hours)**
Adam Cummings	40
Julie Hernandez	35
Alex Kulvivat	12
Mokin Lee	20
Edban Watt	24
Total	131

Table 4: Estimated manufacturing time per team member

Machine	**Time per Assembly (minutes)**	**Total Time (minutes)**
4-axis CNC	15	120
Waterjet	39	312
Total	54	432

Table 5: Time of use for machines requiring extra cost

Expense	**Cost ($)**
Manufacturing Time	13100
Beam Splitters	2715.66
Mirrors	501.39
Nuts and Bolts	43.19
Aluminum for Reflectivity Box	103.72
Shim Stock	29.44
Aluminum for Spacers	3.26
Steel for Shields	14.99

Steel for Front Plates	108.39
Machine Time	1800
Total	18420.04

Table 6: Estimate of all manufacturing expenses

If the system were to be scaled to make 1000 models, a finishing operation could be added to the 4-axis CNC code to eliminate the need for cutting and finishing the parts on a mill. The CNC machine could also be programmed to tap the holes to prevent the need for manual tapping. For the front plates, a program could be written to drill the holes. The shields could be made out of steel L stock if there were any off-the-shelf stock in the proper dimensions. If not, multiple shields could be bent at once before being cut into individual shields. The shields were waterjet cut during manufacturing to provide sharp interior corners, but due to the difficulty of bending the shields exactly along the cut, this cutout was increased in size using a mill after bending. Therefore, the waterjet cutting step can be eliminated for greater scale manufacturing. If a greater number of spacers were needed, they could likely be purchased off the shelf, or washers of a comparable size could be purchased and stacked to the proper height. Lastly, a punch could be created to cut the tabs to the proper size.

Team Member	**Development Time (hours)**
Adam Cummings	62.5
Julie Hernandez	86
Alex Kulvivat	52
Mokin Lee	85
Edban Watt	69
Total	354.5

Table 7: Estimates of time spent by each team member developing the design

Table 7 contains the amount of time spent by each team member developing the design and making manufacturing plans. This time does not include time spent manufacturing, but does include team meetings, meetings with the sponsor, concept generation, research, selection of materials, generation of CAD and drawings, and analysis. The time included in this table is not included in table 6 for manufacturing costs and will not change based on the number of assemblies produced.

TEST PLAN AND RESULTS

From the initial set of hardware requirements provided by the sponsor, the team set forth a list of design specifications, listed in Table 2.

The testing methods proposed at the time of drafting the specifications were to use a CCD camera to measure the intensity of light received at the target end of the light relay, and to use a laser with a diffraction grating to test the operational wavelengths of the light path with the optics installed.

While no quantitative tests were held pertaining to the design specifications listed in Table 2, several procedures were undertaken either by the design team or the designated engineers at the LLE to ensure that all iterations of the final product were functional.

First, to ensure that the product met the required light efficiency, a mathematical relationship between the distance that the light would travel in the light relay and the light efficiency was established for a given hardware design, as shown in Eqn. (1)

$$\epsilon = \frac{\pi}{16}\left(\frac{d_b}{L}\right)^2 \quad (1)$$

where d_b is the diameter of the backlighter opening and L is the distance of the light path within the light relay. The light efficiency originally set to be tested as a percentage would now be tested as a distance. Any design proposed thereafter, the light path distance, was used to verify its validity.

Taking into account the reflectivity of the interior surface of the light relay itself, it was concluded with confidence that the light efficiency specification would be met since the light reflected from the interior surface of the light relay would only lessen the dissipation effects represented by the inverse-square relationship in Eqn. 1. However, confidence in the mathematical calculations is not the same as passing a controlled test experiment that yields a comparable numerical value. Despite the laser experiment at the LLE being successful, it cannot be said that the light efficiency specification was verified using a test. The implementation of tests in the overall design process is discussed further in the designated section.

Similar to the first specification, no quantitative test was verify the operability of the design in the given maximum and minimum wavelengths. However, given that the mirrors and the beam splitters involved in the design were not specifically designed to work on a narrow band of wavelengths, it was understood that the fully assembled light relay with its mirror and beam splitter would be functional within the specified range of wavelengths, especially since the given range is very similar to that of the wavelength of visible light.

After the first iteration of the hardware was completely manufactured and assembled, the part was sent to the LLE to undergo some preliminary fit-and-function testing, which was carried on with specifications that were not given to the team during the time of the initial drafting of the specifications. More iterations of the hardware were manufactured and assembled only after the confirmation from the LLE that the design fit and was functioning.

The integrity of each assembly was examined qualitatively, as discussions arose relating to the possibility of breakage during the setup of the laser experiment due to random motions encountered in the mounting the hardware. Prior to delivering the finished reflectivity boxes to sponsor, each reflectivity box was assembled with a complete set of all the tabs, spacers, and the optics involved, and was vigorously shaken after being put in a plastic bag. The random motions that the assembly was put through were akin to a random vibration test with a range of motion that was more extreme than what would be encountered during the mounting process. It was made sure all the assemblies were intact before being given to the sponsor, with each assembly being tested with a different combination of tabs and spacers.

The functionality of the final product was fully verified after the first experiment shot at the LLE. A picture of the hardware after the first shot is shown in figure 11. The scorched DAC aperture in the front plate proves that the energy from the laser was guided through the light relay, which verifies that the relay fulfilled its most primitive function of relaying light.

A visual representation of the data collected from the shot day experiment is shown in figure 12. Given that it is a plot of how the intensity of the different wavelengths vary through time. With the pulse being well within the 450 nm to 750 nm range laid out in the design specifications, it could be stated with confidence that the final product was indeed successful in meeting the design specifications.

A fish scale test was done to ensure that the mirror and beam splitter would be intact. Mechanical analysis was done considering that at any given stage of the laser experiment, the tabs would not have to withstand a load larger than the weight of the individual optic, and the results were verified through a fish scale test.

Tab Placement	**Critical Deformation (mm)**	**Load from optic weight and FS (N)**	**Load for critical deformation (N)**
Mirror	6	0.122	11
Beam Splitter	3	0.068	5.5

Table 8: Fish scale test results for tabs.

Critical deformation was defined as the length the tabs would have to deflect such that the optic would no longer be held in place i.e. thickness optics. Since the load required to deflect the tab to its critical dimension was roughly 2 orders of magnitude larger than the applied load, this ensures that the optics would be intact.

INTELLECTUAL PROPERTY

The design is not patentable, since it does not present a novel idea and it draws inspiration from a preexisting design, which was previously used for similar experiments. Although the design created for this project has extensive modifications from the original design, there are no changes in the functionality of the assembly. Using mirrors and beam splitters to relay light is a commonly implemented process, and an obvious one for experts in the field. Therefore, it is not a novel idea.

No similar patents were found for this design, but a category that this design could fall into would be G02B17/00 - Systems with reflecting surfaces, with or without refracting elements. The corporation with the most patents under this category is キヤノン株式会社 (Canon Japan). The top three inventors with the most patents in this category are 方涛, 吴慧军, and 徐俊峰.

SOCIETAL AND ENVIRONMENTAL IMPLICATIONS

The main ethical issue that stems from this project is the lack of quality control when producing multiple identical assemblies. Due to time constraints, not all components underwent testing. Measurements from each component, as well as assemblies were not collected. Obtaining this information is crucial in determining manufacturing variability, estimating and reducing errors.

The main materials used for this project were stainless steel 304 and Aluminum 6061. An environmental advantage of these materials is that they are 100% recyclable. When handled in their solid state, the materials used for this project do not present any health hazards. However, the dust and fumes produced from cutting, milling, and grinding these materials can present health and environmental hazards. Powder, and residues from machine these materials, should be disposed of properly, to avoid entry to public waters and sewers as they can be hazardous to aquatic environments.

The components of the final assembly undergo extensive manufacturing process, which require lots of energy and resources. If the number of assemblies manufactured was scaled up, different processes would need to be implemented to speed up manufacturing time and reduce energy consumption.

RECOMMENDATIONS FOR FUTURE WORK

If there were an opportunity to further the project, performing quality control tests would be prioritized. This would aid in reducing errors and improving manufacturing processes. Due to time constraints, limited testing was performed on individual components, and assemblies. It would be interesting to collect data on the dimensions and functionality of each component as it could provide insight into variability from manufacturing. Performing additional analysis like six sigma would aid in minimizing errors between assemblies, while could provide insights into process improvement.

The tabs could be modified to be a metal square that screw on to the reflectivity box and apply force due to the force of the screw rather than the spring force it is currently using. This would make the manufacturing process more efficient, and potentially decrease the environmental impact on the project by reducing the amount of material needed for the tabs, as well as the energy from using fabrication equipment. Another modification that could be implemented, make the shield a flat piece that slots in through the front plate and screws into the reflectivity box.

ACKNOWLEDGMENTS

We would like to thank Professor Muir, Professor Mohammad, and Dr. Neel Kabadi for their guidance, as well as Jim Alkins, Chris Pratt and Bill Mildenberger for their help with manufacturing.

Appendix A: Tables

Deliverable	Description
Reflectivity box prototype	3 functioning prototypes of the reflectivity box
Theory of use document	User manual that explains each of the components, the assembly instructions, and other relevant information.
Final product CAD files	The CAD files used in creating the final product for reference and modification.
Design day poster	A poster for design day that summarizes the project.
Final project report	A report that compiles all the necessary information in the design and manufacturing process involved in the project.

Table 1. The major deliverables in completing the project and their descriptions.

Specification	Method of Evaluation	Value	Units
Minimum percentage of light received by the hydrogen sample	Measure the amount of light received at the target using a CCD camera	0.01	Percent (%)
Minimum wavelength of light in range of operation	Laser testing/white light and diffraction testing	450	nm
Maximum wavelength of light in range of operation	Laser testing/white light and diffraction testing	750	nm

Table 2. Design specification descriptions, method of evaluation, and the target values for each specification.

	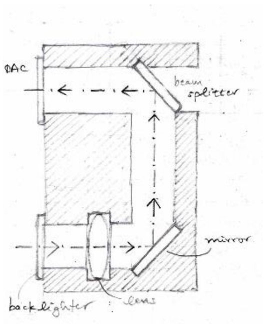	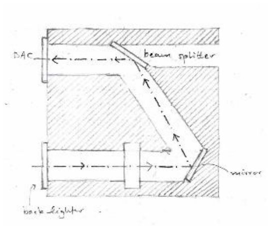	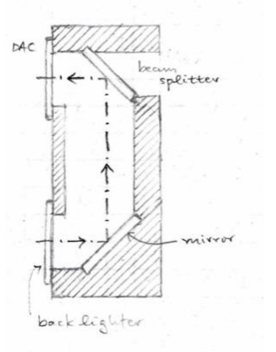	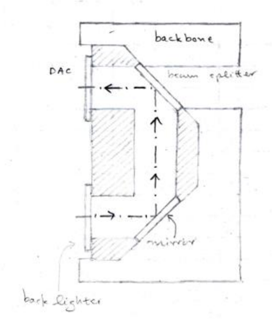
	Concept 1	Concept 2	Concept 3	Concept 4
Ease of Manufacture	0	-	0	+
Expected Light Efficiency	0	+	+	0
Ease of Assembly	0	-	0	+
Debris Protection	0	0	-	-
Total	0	-	0	+

Table 3. Pugh Matrix of Design Concept, Favoring Concept 4

Appendix B: Figures

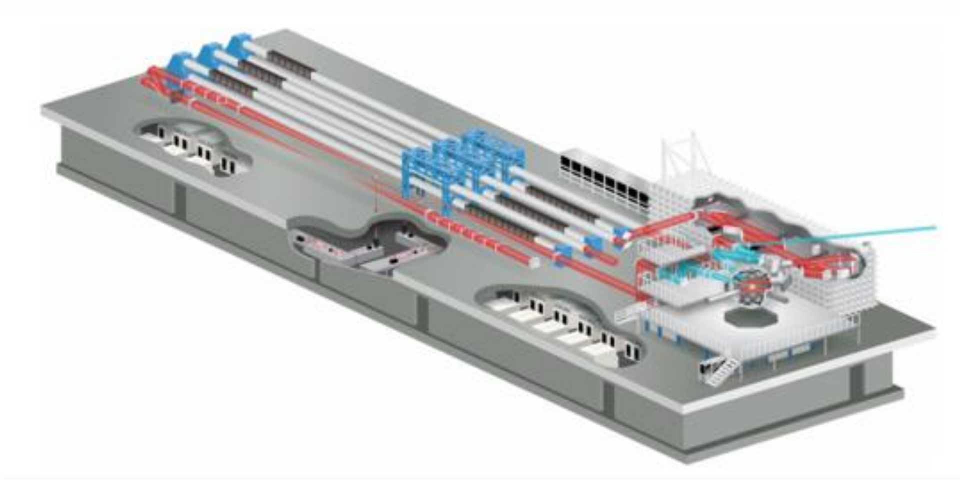

Figure 1. The Omega-EP Laser System consists of four beams driven from one side and is used for planetary experiments.

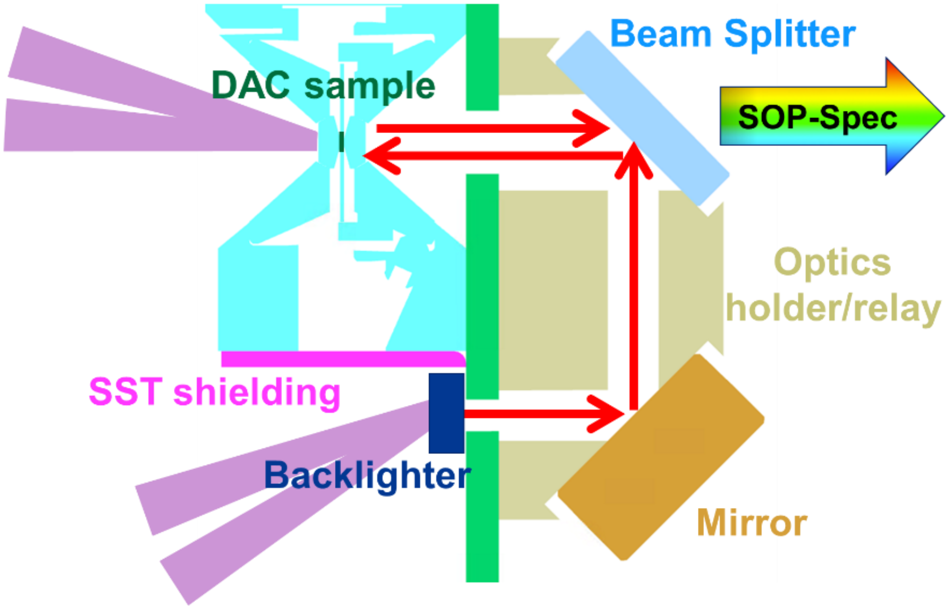

Figure 2. The fundamentals of the reflectivity box entail that light is relayed from the backlight to a mirror, to the beam splitter, to the HED sample, and then back through the beam splitter to the spectrometer.

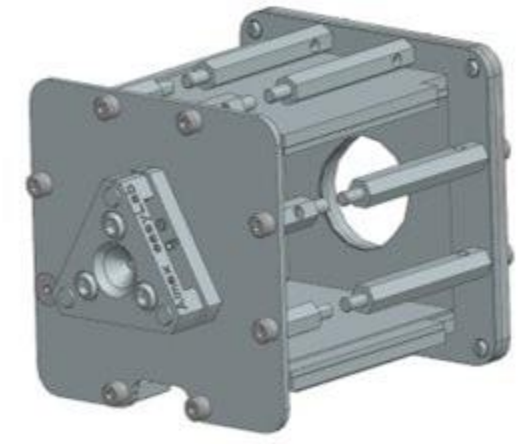

Figure 3. The PXRDIP box is a preexisting assembly in which the reflectivity box will mounted to the front plate. The DAC can be seen mounted to the outside of the front plate.

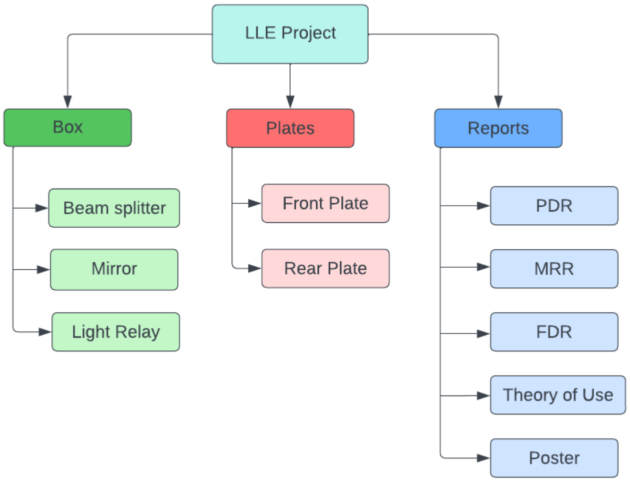

Figure 4. Work Breakdown Structure (WBS) for the project.

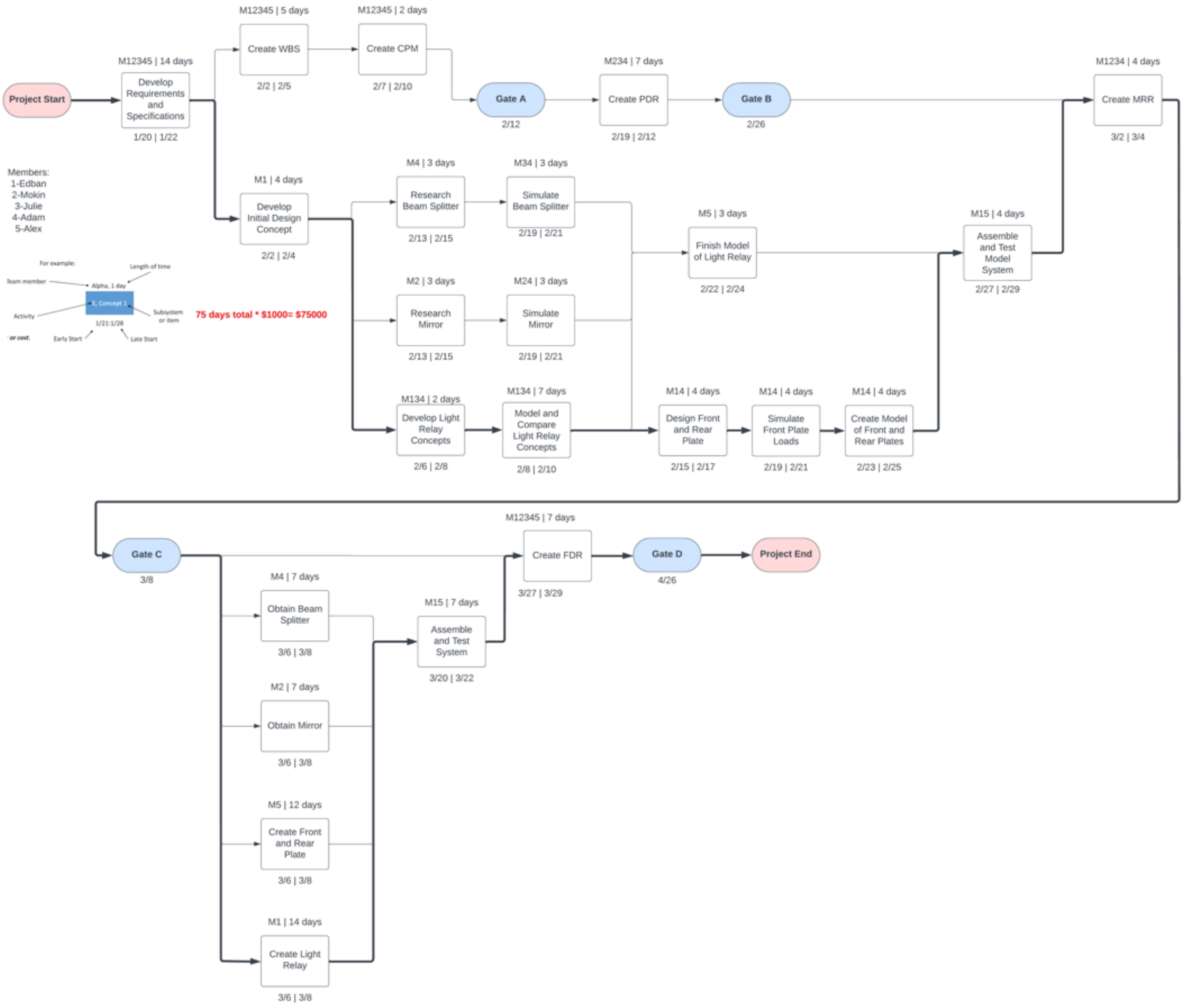

Figure 5. The critical path method (CPM) diagram of the overall project. The critical path is highlighted as a bold line.

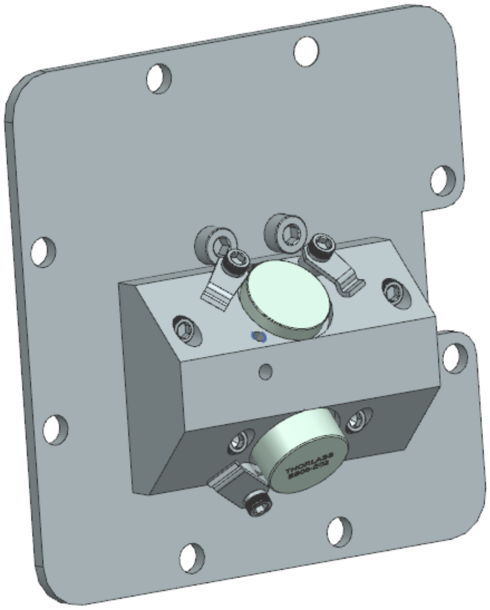

Figure 6. The final design whereas the reflectivity box is fastened directly to the front plate and the optics are held by tabs.

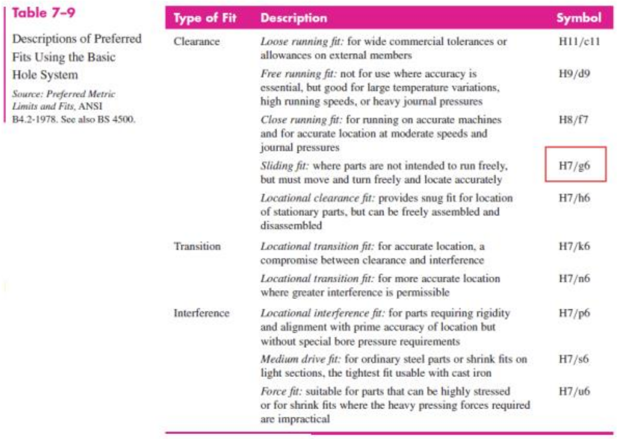

Table 7–9

Descriptions of Preferred Fits Using the Basic Hole System

Source: Preferred Metric Limits and Fits, ANSI B4.2-1978. See also BS 4500.

Type of Fit	Description	Symbol
Clearance	*Loose running fit:* for wide commercial tolerances or allowances on external members	H11/c11
	Free running fit: not for use where accuracy is essential, but good for large temperature variations, high running speeds, or heavy journal pressures	H9/d9
	Close running fit: for running on accurate machines and for accurate location at moderate speeds and journal pressures	H8/f7
	Sliding fit: where parts are not intended to run freely, but must move and turn freely and locate accurately	$\boxed{\text{H7/g6}}$
	Locational clearance fit: provides snug fit for location of stationary parts, but can be freely assembled and disassembled	H7/h6
Transition	*Locational transition fit:* for accurate location, a compromise between clearance and interference	H7/k6
	Locational transition fit: for more accurate location where greater interference is permissible	H7/n6
Interference	*Locational interference fit:* for parts requiring rigidity and alignment with prime accuracy of location but without special bore pressure requirements	H7/p6
	Medium drive fit: for ordinary steel parts or shrink fits on light sections, the tightest fit usable with cast iron	H7/s6
	Force fit: suitable for parts that can be highly stressed or for shrink fits where the heavy pressing forces required are impractical	H7/u6

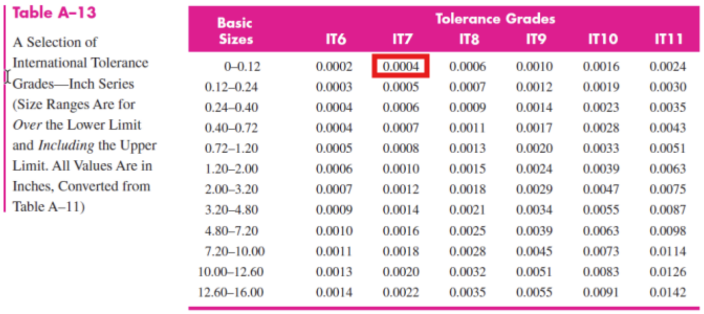

Table A–13

A Selection of International Tolerance Grades—Inch Series (Size Ranges Are for *Over* the Lower Limit and *Including* the Upper Limit. All Values Are in Inches, Converted from Table A–11)

Basic Sizes	Tolerance Grades IT6	IT7	IT8	IT9	IT10	IT11
0–0.12	0.0002	$\boxed{0.0004}$	0.0006	0.0010	0.0016	0.0024
0.12–0.24	0.0003	0.0005	0.0007	0.0012	0.0019	0.0030
0.24–0.40	0.0004	0.0006	0.0009	0.0014	0.0023	0.0035
0.40–0.72	0.0004	0.0007	0.0011	0.0017	0.0028	0.0043
0.72–1.20	0.0005	0.0008	0.0013	0.0020	0.0033	0.0051
1.20–2.00	0.0006	0.0010	0.0015	0.0024	0.0039	0.0063
2.00–3.20	0.0007	0.0012	0.0018	0.0029	0.0047	0.0075
3.20–4.80	0.0009	0.0014	0.0021	0.0034	0.0055	0.0087
4.80–7.20	0.0010	0.0016	0.0025	0.0039	0.0063	0.0098
7.20–10.00	0.0011	0.0018	0.0028	0.0045	0.0073	0.0114
10.00–12.60	0.0013	0.0020	0.0032	0.0051	0.0083	0.0126
12.60–16.00	0.0014	0.0022	0.0035	0.0055	0.0091	0.0142

$$\mathrm{Dmax} = D + \Delta D$$

$$\mathrm{Dmax} = 0.086\mathrm{in} + 0.004\mathrm{in}$$

$$\mathrm{Dmax} = 2.2\mathrm{mm} + 0.1\mathrm{mm}$$

$$\mathrm{Dmax} = 2.286\ \mathrm{mm}$$

$$\mathrm{Dmin} = D$$

$$\mathrm{Dmin} = 2.2\mathrm{mm}$$

Figure 7. Calculations for the proper tolerance to be placed on the clearance hole for the tabs.

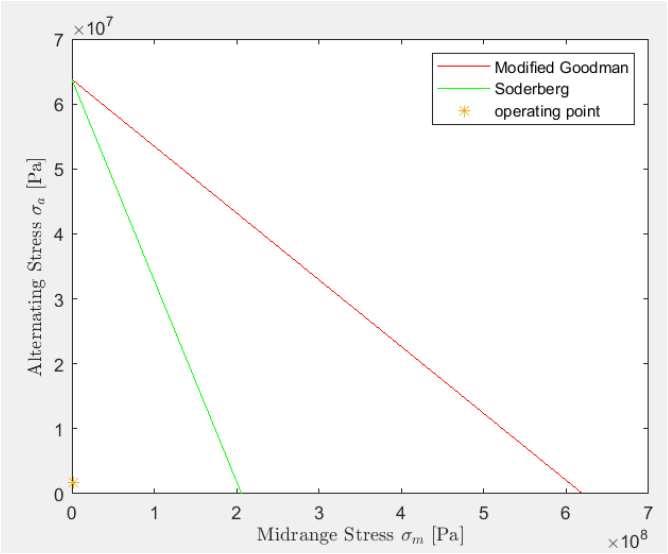

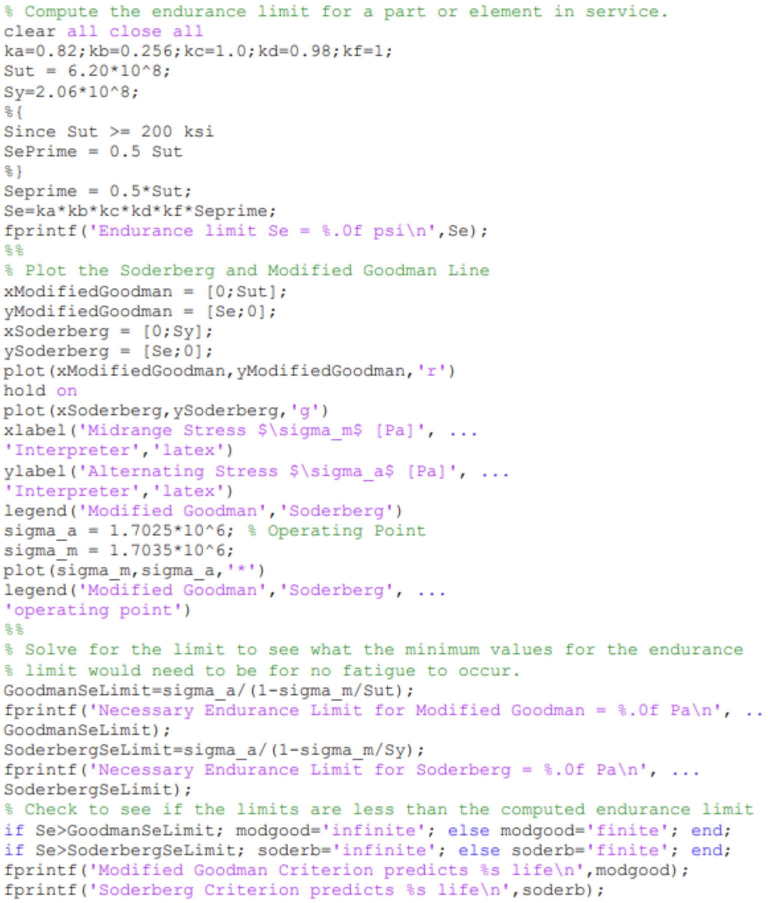

```
% Compute the endurance limit for a part or element in service.
clear all close all
ka=0.82;kb=0.256;kc=1.0;kd=0.98;kf=1;
Sut = 6.20*10^8;
Sy=2.06*10^8;
%{
Since Sut >= 200 ksi
SePrime = 0.5 Sut
%}
Seprime = 0.5*Sut;
Se=ka*kb*kc*kd*kf*Seprime;
fprintf('Endurance limit Se = %.0f psi\n',Se);
%%
% Plot the Soderberg and Modified Goodman Line
xModifiedGoodman = [0;Sut];
yModifiedGoodman = [Se;0];
xSoderberg = [0;Sy];
ySoderberg = [Se;0];
plot(xModifiedGoodman,yModifiedGoodman,'r')
hold on
plot(xSoderberg,ySoderberg,'g')
xlabel('Midrange Stress $\sigma_m$ [Pa]', ...
'Interpreter','latex')
ylabel('Alternating Stress $\sigma_a$ [Pa]', ...
'Interpreter','latex')
legend('Modified Goodman','Soderberg')
sigma_a = 1.7025*10^6; % Operating Point
sigma_m = 1.7035*10^6;
plot(sigma_m,sigma_a,'*')
legend('Modified Goodman','Soderberg', ...
'operating point')
%%
% Solve for the limit to see what the minimum values for the endurance
% limit would need to be for no fatigue to occur.
GoodmanSeLimit=sigma_a/(1-sigma_m/Sut);
fprintf('Necessary Endurance Limit for Modified Goodman = %.0f Pa\n', ..
GoodmanSeLimit);
SoderbergSeLimit=sigma_a/(1-sigma_m/Sy);
fprintf('Necessary Endurance Limit for Soderberg = %.0f Pa\n', ...
SoderbergSeLimit);
% Check to see if the limits are less than the computed endurance limit
if Se>GoodmanSeLimit; modgood='infinite'; else modgood='finite'; end;
if Se>SoderbergSeLimit; soderb='infinite'; else soderb='finite'; end;
fprintf('Modified Goodman Criterion predicts %s life\n',modgood);
fprintf('Soderberg Criterion predicts %s life\n',soderb);
```

Figure 8. Fatigue Analysis showing Modified Goodman and Soderberg plot (left) and MATLAB calculations (right)

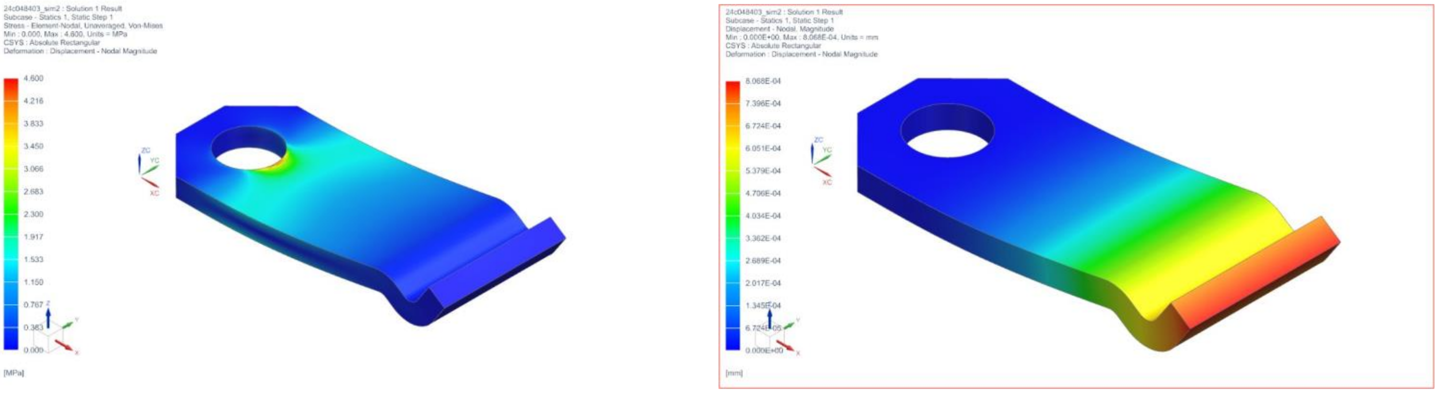

Figure 9. Linear Statics FEA simulation showing Von Mises stress (left) and displacement (right)

$$I = \frac{(mass\ of\ plate)\cdot(L)^2}{12}$$

$$I = \frac{(6.04\cdot10^{-8})\cdot(0.011)^2}{12}$$

$$I = 5.03 \cdot 10^{-13}\ m^4$$

$$F = Weight\ \cdot\ FS$$

$$F = 0.04082331\ N \cdot 3$$

$$F = 0.122\ N$$

$$\delta = \frac{FL^3}{3EI}$$

$$\delta = \frac{(0.122)\cdot(0.010)^3}{3(1.93\cdot10^{11})(5.03\cdot10^{-13})}$$

$$\delta = \frac{1.22\cdot10^{-7}}{0.291237}$$

$$\delta = 4.19 \cdot 10^{-7}\ m$$

$$\delta = 0.000418\ mm$$

Figure 10. Cantilever beam hand calculation to model weight of optics on tab

Figure 11. Image of front plate after the first laser shot. The mirror is coated with aluminum that was blasted through the light relay.

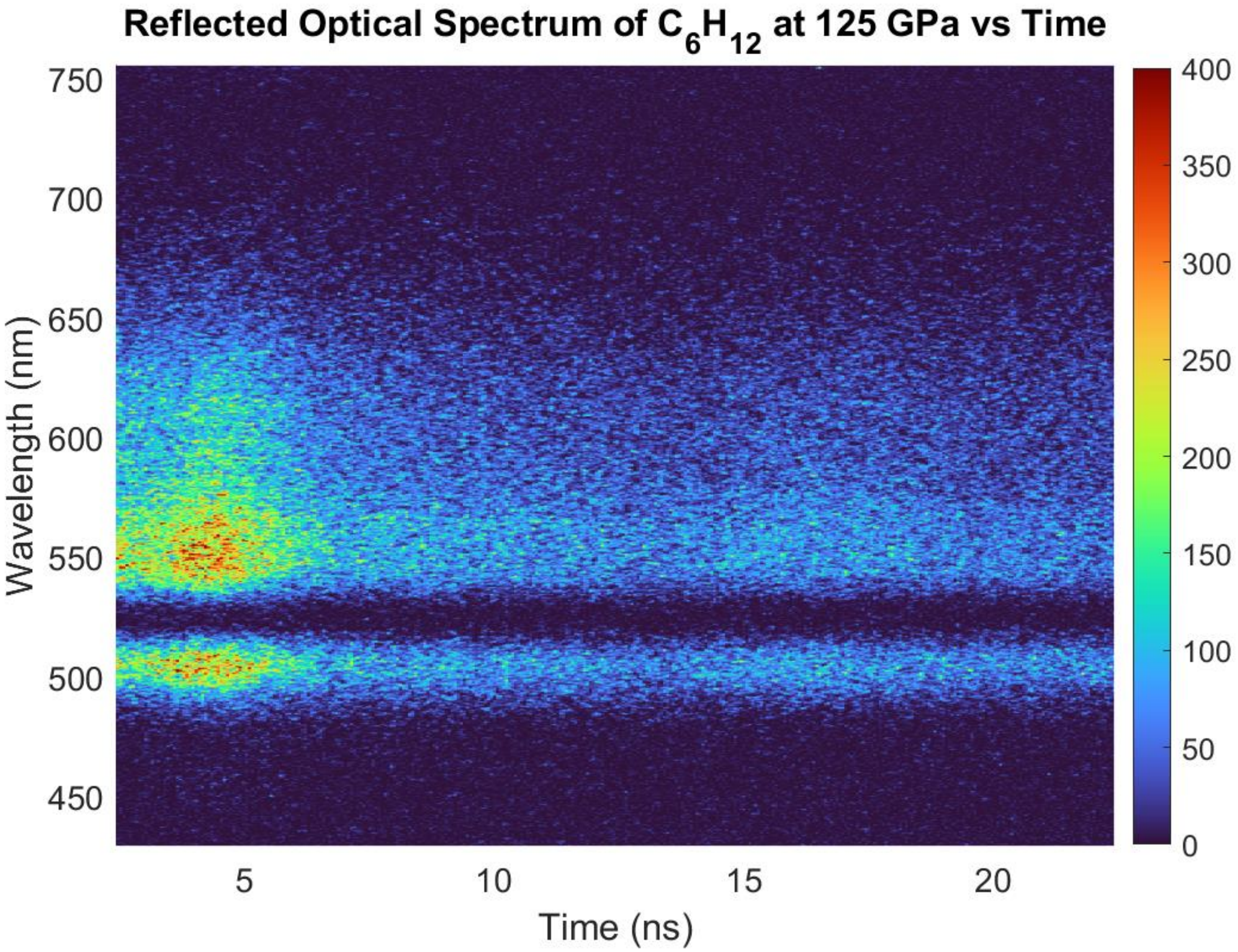

Figure 12. Visualization of data collected from the LLE experiment.

Appendix C: Assembly Manual

Reflectivity Box and Optics Assembly

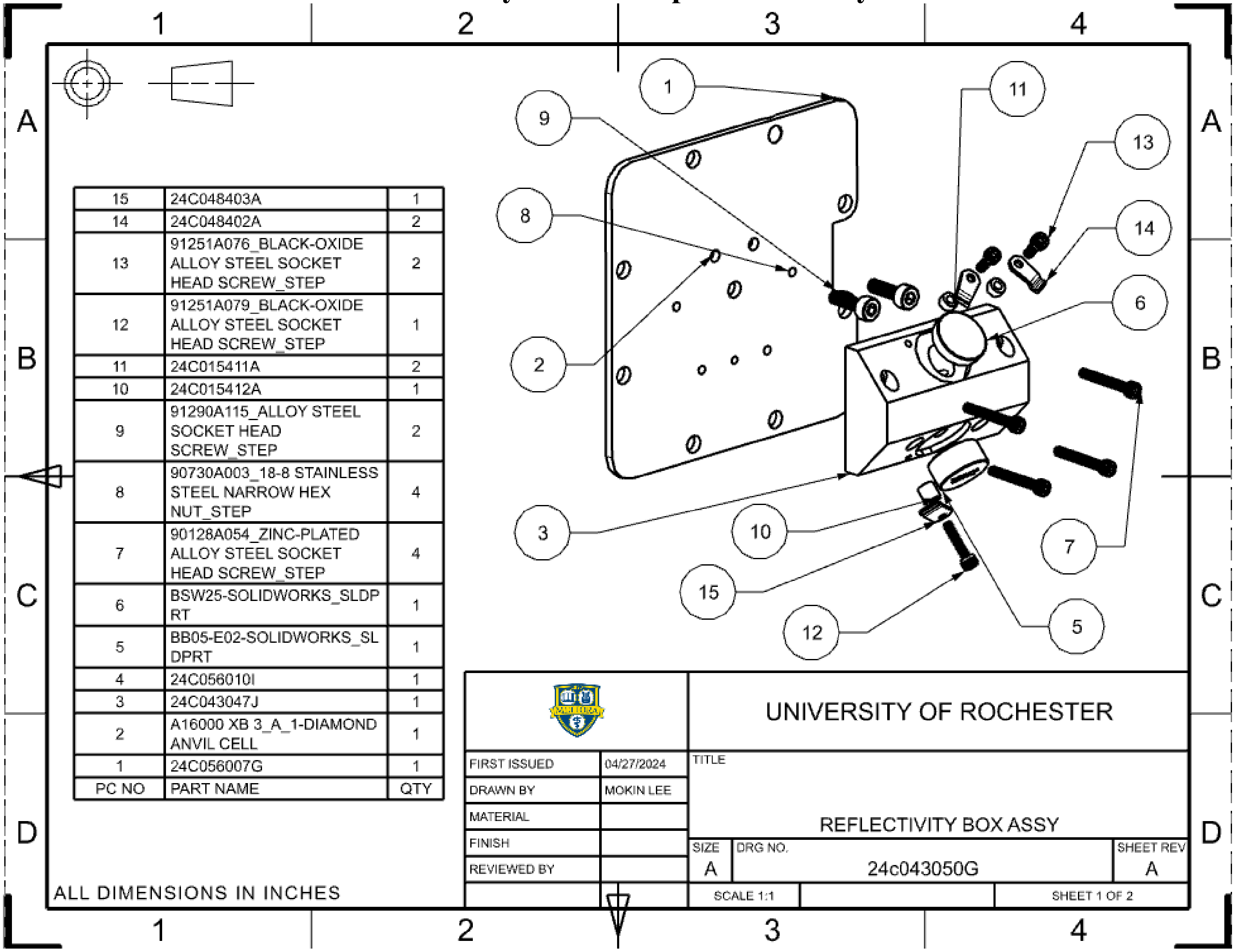

15	24C048403A	1
14	24C048402A	2
13	91251A076_BLACK-OXIDE ALLOY STEEL SOCKET HEAD SCREW_STEP	2
12	91251A079_BLACK-OXIDE ALLOY STEEL SOCKET HEAD SCREW_STEP	1
11	24C015411A	2
10	24C015412A	1
9	91290A115_ALLOY STEEL SOCKET HEAD SCREW_STEP	2
8	90730A003_18-8 STAINLESS STEEL NARROW HEX NUT_STEP	4
7	90128A054_ZINC-PLATED ALLOY STEEL SOCKET HEAD SCREW_STEP	4
6	BSW25-SOLIDWORKS_SLDPRT	1
5	BB05-E02-SOLIDWORKS_SLDPRT	1
4	24C056010I	1
3	24C043047J	1
2	A16000 XB 3_A_1-DIAMOND ANVIL CELL	1
1	24C056007G	1
PC NO	PART NAME	QTY

ALL DIMENSIONS IN INCHES

UNIVERSITY OF ROCHESTER

FIRST ISSUED	04/27/2024
DRAWN BY	MOKIN LEE
MATERIAL	
FINISH	
REVIEWED BY	

TITLE
REFLECTIVITY BOX ASSY

SIZE	DRG NO.	SHEET REV
A	24c043050G	A

SCALE 1:1
SHEET 1 OF 2

Suggested Assembly Order

1. Hold the beam splitter spacer (11) and the beam splitter tab (14) in place and screw them both into the reflectivity box to hold them in place (13). Repeat for both sets of spacers and tabs.
2. Place the beam splitter (6) in its designated spot on the reflectivity box and tighten the screws holding the tabs (13).
3. Hold the mirror spacer (10) and mirror tab (15) in place and screw them into the reflectivity box to hold them in place (12).
4. Place the mirror (5) in its designated spot on the reflectivity box and tighten the screw holding the tab (12).
5. Place the reflectivity box with the optics installed and use the designated screws (7) to hold it in place. Tighten the nuts (8) on the other side of the front plate (1) to fasten the reflectivity box onto the front plate.

Diamond Anvil Cell (DAC) and Shield Assembly

PC NO	PART NAME	QTY
4	90730A003_18-8 STAINLESS STEEL NARROW HEX NUT_STEP	4
3	24C056010I	1
2	A16000 XB 3_A_1-DIAMOND ANVIL CELL	1
1	24C056007G	1

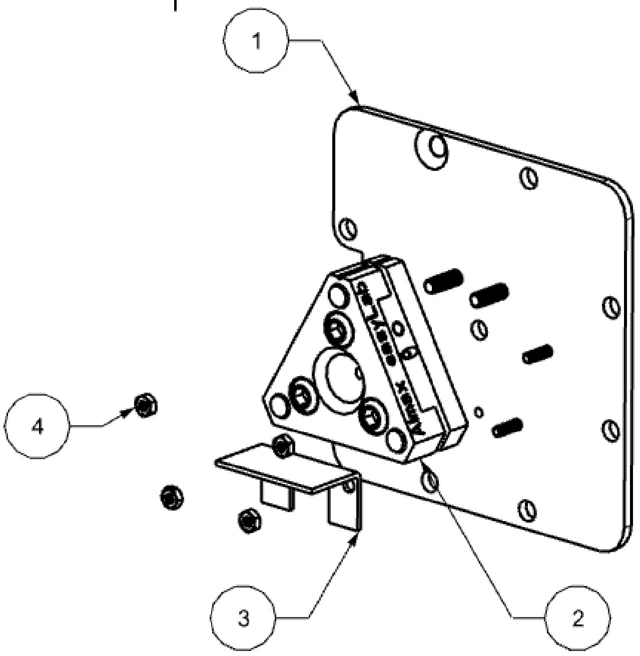

UNIVERSITY OF ROCHESTER

FIRST ISSUED	04/27/2024
DRAWN BY	MOKIN LEE
MATERIAL	
FINISH	
REVIEWED BY	

TITLE
DAC MOUNT ASSY
SIZE A
DRG NO. 24c043050G
SHEET REV A
SCALE 1:1
SHEET 2 OF 2

ALL DIMENSIONS IN INCHES

Suggested Assembly Order

6. Line up the DAC (2) with its screw holes on the plate and use the designated screws (9, from the previous page) from the side of the reflectivity box to hold it in place. Tighten the screws to fasten the DAC to the front plate (1)
7. Line up the shield (3) with the screw holes on the front plate. Send the designated screws through from the reflectivity box and tighten the nuts to mount the shield to the front plate.